

# **Application of green solvents as a replacement of toxic dimethylformamide in the polylactic acid electrospinning process**

Lenka Lovecká\*, Miroslava Kovářová, Dominika Hanušová, Dušan Kimmer, Andrea Poláchová, Vladimír Sedlařík

Tomas Bata University in Zlin, Centre of Polymer Systems, tr. T. Bati 5678, 760 01 Zlin, Czech Republic

\*Corresponding author: [lovecka@utb.cz](mailto:lovecka@utb.cz)

## **Abstract**

Nanofibres based on polylactic acid (PLA) have a wide range of applications, including air filtration. They are prepared by electrospinning using toxic solvents as dimethylformamide. This study focused on the use of green solvents to prepare electrospinnable solutions. It was found that a combination of solvents is necessary. A nozzle electrospinning technique was applied to produce PLA nanofibres from optimised dual (ethyl or methyl lactate with acetone) or ternary (cyclopentanone, acetone and ethyl or methyl lactate) solvent system. The prepared nanofibres were evaluated for morphology and quality of nanofibres (SEM), surface wettability (contact angle), filtration properties (automated filter tester) and pore size and distribution (porometry). Potential changes in the chemical composition and the presence of residual solvent were investigated by FTIR, TGA and headspace analysis. It was found that dimethylformamide can be substituted by green solvents; especially combination of cyclopentanone/ethyl lactate/acetone provides air filtration properties comparable to dimethylformamide/acetone-based systems.

**Key words:** electrospinning, nanofibre, green solvent, PLA, dimethylformamide, air filtration

## **1. Introduction**

Electrospinning is a method of preparing submicron fibres in an electrostatic field that is created between a fibre-forming electrode and a collector. Electrostatic forces give rise to such fibres from a drop of polymer solution located on the electrode, which receives a high voltage. The solvent evaporates as the filament is pulled from the droplet at the electrode to the grounded collector. The resultant nanofibres are deposited on the collector and collecting substrate, respectively [1–4].

The morphologies and diameters of the resulting nanofibres vary in accordance with three primary factors, namely the properties of the solution, the parameters of the process and the given ambient conditions. Optimizing these parameters is necessary to obtain nanofibres that possess specific morphology and well-defined physical and mechanical properties. Extensive study has been devoted mainly to process parameters in this regard, although the properties of the polymer solution are equally important. Another crucial factor is the solvent (or mixed solvent system) applied that significantly affects the properties of the resulting polymer solution, including its electrospinnability. The concentration, conductivity and surface tension of the polymer solution have a considerable effect on the morphology and diameter of the obtained nanofibres.

A wide range of synthetic and natural polymers can be processed by solution electrospinning, including biodegradable polylactic acid (PLA). PLA is promising environmentally friendly biopolymer with desirable physical properties. Nanofibrous structures fabricated from PLA show immense potential in medical applications, e.g. tissue engineering, wound healing and drug release, as well as in industries, such as food packaging [4–9].

Electrospun PLA nanofibres are also applicable in air filtration or purification systems, since they possess a large surface area, high porosity and considerable filtration efficiency, while also boasting the advantage of being biodegradable at the end of their life cycle [10–13].

A suitable solvent is required to prepare an effectively electrospinnable polymer solution. The selection of a suitable solvent necessitates consideration of the desired nanofibre morphology and sufficient process productivity of the small diameter defect-free fibres, as well as the intended application of the nanofibrous material. Solvents utilized in the electrospinning of PLA tend to be toxic, examples being chloroform, dimethylformamide (DMF), dimethylacetamide (DMAc), dichloromethane (DCM), tetrahydrofuran (THF), hexafluoro-2-propanol (HFIP) and N-methyl-2-pyrrolidone (NMP), etc. [14–16]. Apart from possessing a risk to the health and safety of humans, they are also harmful to the environment. The most widespread dipolar aprotic solvents, namely DMF, DMAc and NMP, are at the forefront of concern since they incur risks to health such as reproductive toxicity. These concerns have been expressed by the European Union in its Registration, Evaluation, Authorization, and Restriction of Chemicals (REACH) legislation, categorizing them as “substances of very high concern” (SVHC). The aim is to replace them with less hazardous substances if “technically and economically feasible alternatives” are deemed to exist. Further restrictions on the utilization of these substances shall be imposed over time.

According to Annex XVII of REACH, the use of DMF has been restricted since December 2023, underlining the critical need to find alternatives to it [17, 18].

So called “green solvents” can be used to replace DMF and other hazardous solvents. The concept of green solvents reflects the intention to minimize the environmental impact from the production of chemicals to their disposal. Each solvent is scored using the EHS (environmental, health and safety) indicator, adding up the scores for the water hazard, persistence, chronic toxicity, irritancy, acute toxicity, reactivity, fire and explosion hazard, and release potential that characterise each compound. The production phase, usage, eventual recycling, and disposal of the solvent is characterised by the cumulative energy demand (CED), which can be determined by a life cycle assessment (LCA). The CED and EHS indicators together therefore express how green the solvent is. Lower score means less problematic or greener solvent [19–24].

The selection of a suitable alternative solvent is an important parameter in electrospinning. The solvent has to have the capacity to dissolve the polymer and resulting solution has to be processable into fibres in an electrostatic field. A number of solvents from biological sources are applicable as green alternatives to DMF in the preparation of PLA solutions, e.g. Cyrene (dihydrolevoglucosenone),  $\gamma$ -valerolactone (GVL), Rhodiasolv Polarclean (methyl 5-(dimethylamino)-2-methyl-5-oxopentanoate). N-butylpyrrolidinone (NBP), which is absent of reproductive toxicity, also appears to be suitable as a substitute dipolar aprotic solvent. The high boiling point of all such solvents means they are considered as safe. For example, they are often utilized in a phase separation process of the polymer membranes fabrication [25–27]. Although the low evaporation rate they exhibit somewhat limits their applicability in electrospinning [28–31], certain green solvents have nevertheless attracted attention in nanofibre production, notably cyclopentanone (CPO), ethyl lactate (EL) and methyl lactate (ML). They have the advantage of reasonable cost and relatively easy recyclability, which are aspects valued in the industrial production of PLA nanofibres guided by strict waste management conditions [32–34].

It is quite commonplace to utilize mixtures of solvents in the preparation of electrospinning solutions, their properties mutually acting to bring about the desired result. Blends of solvents are also applied in order to produce nanofibres in more environmentally friendly manner with reduced risk to health. Electrospinning of PLA works well when DMF is utilized, yet it is still possible to fabricate high-quality nanofibres free of defects and deformation by using a solvent system wherein up to 20% of DMF is substituted by more

environmentally acceptable acetone [35–37]. In this respect, Casasola et al. [14] investigated the applicability of acetone in the electrospinning of PLA and combined it with another toxic solvents such as DMAc. They prepared defect-free nanofibres from solutions of PLA in DMF/acetone at a 40:60 ratio or DMAc/acetone at a 50:50 ratios, and even from just pure acetone. The structures contained nanofibres with quite large diameters. This could cause a problem when applied to air filtration.

The main research aim of this study was to verify the possibility of preparing high quality PLA nanofibers from green solvents-based solutions by electrospinning. Such nanofibrous materials should provide similar air filtration properties to conventional PLA nanofibrous membranes prepared from toxic solvents. Based on optimization tests, an alternative (green) solvent system was searched for to provide polymer solutions with good electrospinnability. Subsequently, the prepared nanostructures were compared with nanofibers fabricated from a solution of PLA in DMF, a widely used toxic solvent. A nozzle-based electrospinning system was used for this purpose.

The electrospinnability of the solutions was studied with respect to the properties of the polymer solutions and the effect of alternative solvents on the morphology and diameters of the nanofibers, as well as on the possible residual solvent content in the nanofibrous structures. The filtration properties of the prepared nanofibrous membranes were subsequently compared based on filtration tests with sodium chloride-based aerosol.

## **2. Materials and Methods**

### **2.1 Materials**

Cyclopentanone (CPO), ethyl lactate (EL), methyl L-lactate (ML),  $\gamma$ -valerolactone (GVL), N, N-dimethylformamide (DMF), N-butylpyrrolidinone (NBP) and Cyrene were purchased from Sigma-Aldrich (Germany). Acetone was supplied by Lach-Ner (Czech Republic). Sodium tetraborate decahydrate and citric acid were sourced from Ing. Petr Švec - PENTA (Czech Republic). All chemicals used were in purity for analysis. PLA (Ingeo biopolymer 4060D) was obtained from NatureWorks (USA). The nonwoven textile used as collecting support (polypropylene spun-bond, basis weight 30 g.m<sup>-2</sup>) was purchased from PFNonwovens Czech (Czech Republic). All the chemicals were used as delivered.

### **2.2 The Electrospinning Process**

The nanofibres were prepared on a SpinLine 40 electrospinning device (SPUR, Czech Republic), with simultaneous drying of the interior of the equipment to a relative humidity of 25–30% by a Munters ML180 (Munters, Germany) dryer. A voltage of 65–75 kV was applied to spin a drop of polymer solution from the test stick, with a distance of 18 cm between the electrodes. For the continuous process of nanofibres preparation an eight-nozzle moving system with a polymer solution dosing unit was employed. The nanofibres were collected on a polypropylene nonwoven support textile.

### 2.3 Characterization of the nanofibrous layer

#### 2.3.1 Scanning electron microscopy

The structure, surface morphology and fibre diameters of the nanostructured materials were evaluated by SEM (scanning electron microscopy; Phenom, Phenom-World, Netherlands). Samples of the nanofibrous materials were coated with a thin layer of a gold and palladium alloy to increase their electrical conductivity before SEM imaging.

#### 2.3.2 FTIR spectroscopy and thermogravimetric analysis (TGA)

The chemical composition and presence of residual solvents in the prepared nanofibres were determined by FTIR spectroscopy. Fourier transform infrared attenuated reflectance (FTIR-ATR) was carried out to obtain spectra for all the materials, on a Nicolet iS5 unit (Thermo Fisher Scientific, USA). The instrument was equipped with a Ge crystal for determination of structural changes in chemical bonds. It was set to a range of 600–4000  $\text{cm}^{-1}$  and a resolution of 4 and 64 scans, with subsequent analysis in OMNIC software (Thermo Fisher Scientific, USA).

The composition of the nanofibres was quantified by thermogravimetric analysis (20–600°C, 10°C  $\text{min}^{-1}$ , under a nitrogen flow of 50  $\text{mL min}^{-1}$ ), on a TA Q500 thermogravimetric analyser (TA Instruments, USA); relative standard deviation of measurement equalled 1%.

#### 2.3.3 HS-SPME-GC-MS analysis

The presence of extractive residual solvents was gauged on an Agilent 7200 system, consisting of an Agilent 7890B gas chromatograph equipped with a multimode inlet and PAL RSI 85 for automated headspace solid-phase microextraction (HS-SPME) and direct injection and quadrupole time-of-flight mass spectrometry (Q-TOF). Two HP-5MS UI columns (15 m  $\times$  25 mm, film thickness of 0.25  $\mu\text{m}$ ) were operated in scan detector mode

(40-400 m/z). Analytes were adsorbed on divinylbenzene/carboxen/polydimethylsiloxane (DVB/CAR/PDMS) fibre and conditioned at 270°C for 30 minutes. SPME fibre was desorbed in the GC-MS inlet at 250°C for 5 minutes, applying split mode injection. The oven temperature program was as follows: an initial stage transpired at 40°C for 3 minutes, followed by a heating rate of 4°C min<sup>-1</sup> to 100°C, and then a rise to 200°C at 6°C min<sup>-1</sup>. Helium was applied as the carrier gas at a flow rate of 1.0 and 1.2 mL min<sup>-1</sup>, while the detector temperature was 230°C.

#### *2.3.4 Nanofibrous layer wettability*

Measuring the contact angles of a material provides data on the hydrophilicity or hydrophobicity of nanofibrous layer surface. The wettability of the given surface was determined by measuring static contact angles with apparatus equipped with a charge-coupled device (CCD) camera to obtain digital images of the drop of a testing liquid (SEE System; Advex Instruments, Czech Republic). A photograph of the droplet was taken approximately 1 second after release of the liquid from a micropipette. Samples were tested with a water droplet equalling 3 µl in volume. A mean value was calculated from five such tests. SEE System software was used to analyse the images and determine values for contact angles.

#### *2.3.5 Determination of filtration properties*

The Automated Filter Tester 3160 (TSI, USA) was employed to discern the filtration properties of the nanofibrous layers. Measurements were carried out on circular samples with an area of 100 cm<sup>2</sup> at the temperature of 25°C and relative humidity of 30%. The filtration properties of the nanofibrous layers were determined according to EN 1822-1, applying a NaCl-based aerosol at a flow rate of 30 l min<sup>-1</sup>. The measurements were carried out over a particle size range of 20 to 400 nm. The filtration efficiency, pressure drop and MPPS (Most Penetrating Particle Size) of the filter media were subsequently evaluated using Certitest software.

#### *2.3.6 Porometry*

The pore sizes of the nanostructured materials were characterized by porometry on a porometer (SPUR, Czech Republic), in accordance with ASTM F316-03 (2011). Galpore (Porometer, Belgium) was applied as the wetting fluid. Dry and wet tests were performed on three circular samples cut from the given materials and average values were reported. The

porometer measurements indicates mean and maximum pore diameters and value for dry air permeability. Pore size distribution could also be determined from such measurements.

### 3. Results and discussion

Green solvents, generally considered alternatives to DMF, were selected for experiments. Their ability to dissolve PLA and additives that increase the electrical conductivity of electrospinning solutions (a mixture of sodium tetraborate decahydrate and citric acid referred to as BC at a ratio of 1:3) were investigated. The experiments involved preparation of 16% solutions of PLA and 18% solutions of the conductivity-enhancing additive in the given solvents. Dissolution occurred over a period of 16 hours at laboratory temperature (25°C). When it proved impossible to prepare a solution under such conditions, the temperature for dissolution was raised to 40–60°C for 8 h. The results are detailed in Table 1.

Table 1 Selected solvents, their properties and the solubility of PLA and the conductivity-enhancing additive (BC)

Solvent	PLA solubility	BC solubility	Relative evaporation rate (ref. DMF)	Vapour pressure, 25°C (hPa)
Cyrene	+	-	14.90	0.14
NBP	+/-	+	63.70	0.13
GVL	+	-	4.60	0.44
Ethyl lactate	+/-	+	1.67	1.55
Methyl lactate	+/-	+	1.00	4.67
Cyclopentanone	+	-	0.38	15.20
Acetone	+	-	0.01	308.51
DMF	+/-	+	1.00	4.93

+ dissolved, +/- partially dissolved, - not dissolved

When selecting a suitable solvent for preparing nanofibres by electrospinning, it is necessary to focus on the properties of the solvent itself, specifically the rate of evaporation. This not only influences the electrospinning process, but also the properties and quality of the resultant nanofibres. The solvent has to exhibit a sufficiently high rate of evaporation. The nanofibrous layer should not contain any residual solvent that would affect the structure of other nanofibres deposited on the substrate. Utilizing a solvent that evaporates slowly could lead to the occurrence of electrospray. The selection of the solvent can be guided by the evaporation rate or vapour pressure values of the solvent specified by the manufacturer (Table 1). In order to compare the green solvents tested with DMF, the relative rate of evaporation (ER) was determined. This represents a ratio of the time required for the total amount of tested solvent to evaporate ( $t_s$ ) to that for the DMF reference solvent ( $t_R$ ) at 25°C; see Equation 1 below:

$$ER = \frac{t_S}{t_R} \quad (1)$$

Based on the data presented in Table 1, it was decided that the solvents Cyrene, NBP and GVL have low evaporation rates and therefore were deemed unsuitable for preparing PLA solutions for electrospinning of nanofibres.

Simultaneous dissolution of the polymer and conductivity-enhancing additive is necessary to obtain a nanofibre-forming polymer solution. Since the selected solvents did not meet this prerequisite, attention turned towards combining them instead. The chosen reference system comprised a proven solution of PLA in DMF and acetone at the ratio of 80:20 (16% PLA solution, 0.2% of conductivity enhancer, conductivity ca 140  $\mu\text{S cm}^{-1}$ ). In order to ensure sufficient electrospinnability of the polymer solution, changes in the ratio of solvents, polymer and conductivity enhancing additive were made in the optimization stage. Table 2 shows the composition and conductivity of the solutions chosen for electrospinning using the test stick. The process was carried out under conditions of: voltage 60–75 kV, electrode distance 18 cm, relative humidity 30% and temperature 25°C.

Table 2 Solvent systems and ratios, PLA concentrations and the electrical conductivity of optimized solutions selected for testing

<b>Solvent system, ratio</b>	<b>PLA solution concentration (w/w %)</b>	<b>Conductivity-enhancing additive (BC) content, per solution (w/w %)</b>	<b>PLA solution conductivity (<math>\mu\text{S cm}^{-1}</math>)</b>
EL/acetone 80:20	13	0.8	74.2
EL/acetone 60:40	13	0.8	56.4
EL/acetone 70:30	13	0.8	70.8
EL/acetone 70:30	13	1.6	142.3
EL/acetone 70:30	13	2.4	217.0
ML/acetone 70:30	13	0.8	101.6
CPO/EL/acetone 60:10:30	13	1.6	91.4
CPO/EL/acetone 58:12:30	13	1.6	94.6

The effect of the solvent ratio of ethyl lactate/acetone and the content of conductivity enhancing additive in the PLA solution on the nanofibre structure is presented in the SEM images in Fig. 1. A low level of acetone content (20%) resulted in thin PLA nanofibres, which showed evidence of distinct defects – beads (Fig. 1a). Raising the amount of acetone (40%) in the solvent system did not improve the problem (Fig. 1b). The resultant nanofibres proved thicker and brittle with inhomogeneous deposition. The best results were obtained for a 13% PLA solution with an EL/acetone ratio of 70:30.

Generally, a higher content of conductivity-enhancing additive contributes to the formation of thinner nanofibres. In this case, however, the opposite effect was seen, so no further rise in

concentration of conductivity-enhancing additive was tested. The PLA solution based on the EL/acetone solvents at the ratio 70:30 and the conductivity enhancer content of 0.8% demonstrated the best results (see Fig. 1c).

Since the properties exhibited by ethyl lactate and methyl lactate are similar, the optimal composition of the ML/acetone-based electrospinning solution is also similar. The optimal solvent ratio is 70:30 (ML/acetone) and the content of conductivity-enhancing additive is 0.8% (see Fig. 1f).

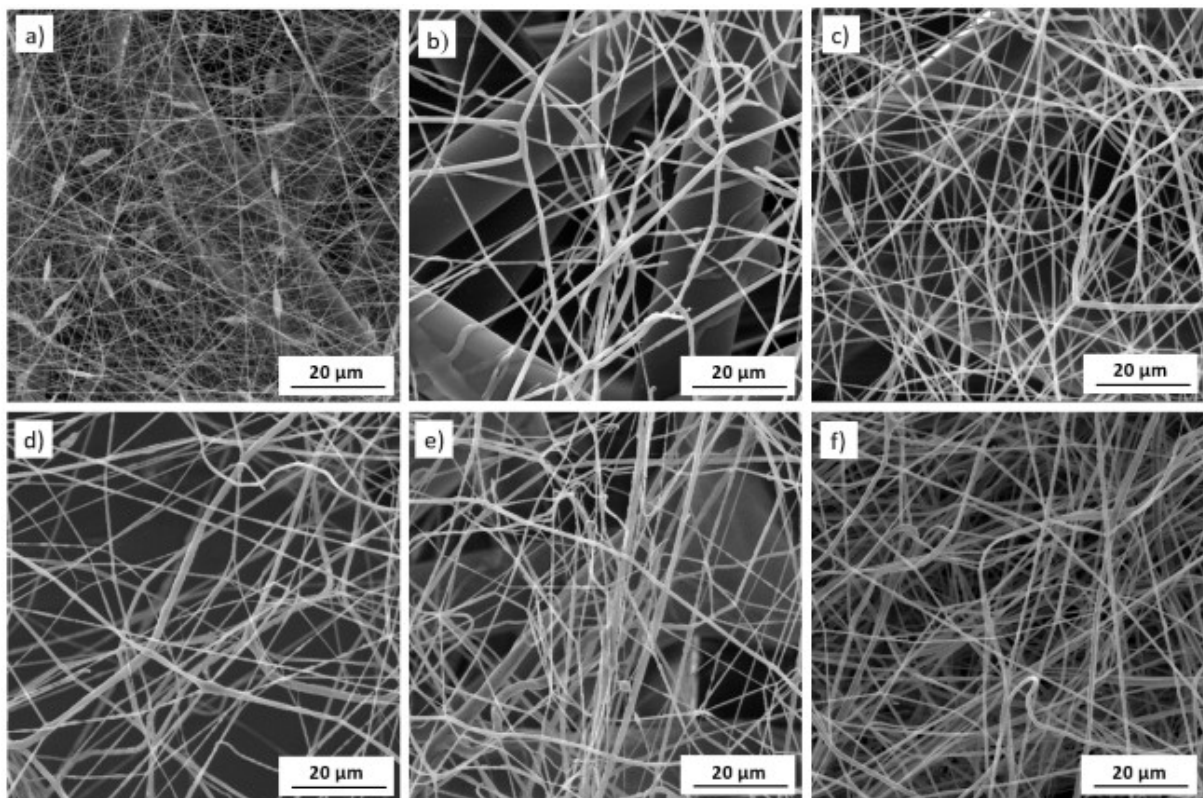


**Fig. 1** SEM images (magnification 1500 $\times$ ) of nanofibres prepared from 13% (w/w) solution of PLA in different solvent systems or with differing content of the conductivity-enhancing additive (BC): (a) EL/acetone 80:20, 0.8% BC; (b) EL/acetone 60:40, 0.8% BC; (c) EL/acetone 70:30, 0.8% BC; (d) EL/acetone 70:30, 1.6% BC; (e) EL/acetone 70:30, 2.4% BC and (f) ML/acetone 70:30, 0.8% BC

The composition of the solvent system containing cyclopentanone was somewhat different. PLA dissolves well in a combination of CPO and acetone, but the insolubility of the conductivity-enhancing additive presented an issue herein. For this reason, a portion of the CPO in the system was replaced by ethyl lactate, in which the additive was soluble. It is necessary to use only such a quantity of the conductivity enhancing additive solution in the third solvent that the additive does not precipitate out of solution when mixed into the base solvent system. By testing various solvent ratios in the PLA solution, the optimum ratio of CPO, EL and acetone was discerned to be 58:12:30 (Figs. 2a, b).

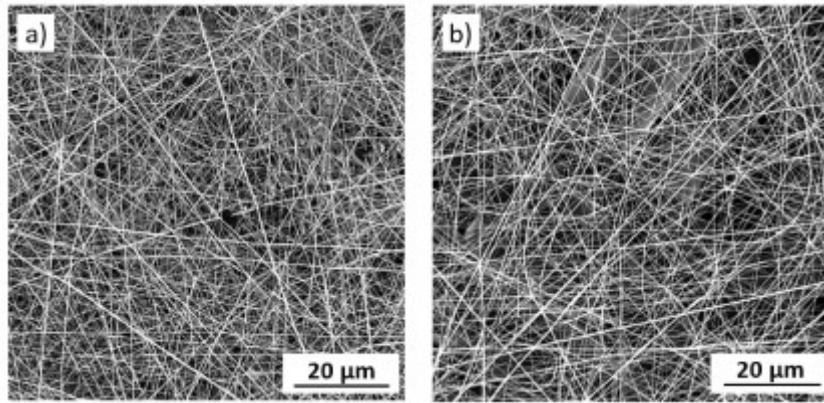


**Fig. 2** SEM images of nanofibres prepared from 13% (w/w) solution of PLA in CPO/EL/acetone at the ratios of (a) 60:10:30 and (b) 58:12:30; content of the conductivity-enhancing additive (BC) 1.6%; at magnification 1500×

After optimizing the composition of the PLA solutions in the green solvents, their extent of electrospinnability was verified in a continuous process using a moving electrospinning unit equipped with eight nozzles. A quantity of 100 g of each PLA solution was prepared by stirring on a magnetic stirrer at laboratory temperature for 16 h. The viscosity ( $\eta$ ) and electrical conductivity ( $\chi$ ) of the solutions were measured prior to electrospinning; the solutions were electrospun at a voltage ( $U$ ) of 60–75 kV onto a polypropylene non-woven fabric moving over a collection electrode. The speed of substrate movement was varied between 0.1–0.5 m min<sup>-1</sup> (5 speeds). Spinning currents ( $I$ ) were also recorded during the tests. Table 3 summarizes the properties of the polymer solutions and given process conditions.

Table 3 Properties of the polymer solutions and process conditions for preparing nanofibres on a nozzle-based electrospinning unit

PLA solution	Solution parameters				Process parameters				
	$c_{PLA}^a$ (w/w %)	$\eta$ (Pa s)	$\chi$ ( $\mu$ S cm <sup>-1</sup> )	$c_{BC}^b$ (w/w %)	$U$ (kV)	$I$ ( $\mu$ A)	Dosage (mL min <sup>-1</sup> )	Electrode distance (cm)	Support textile speed (m min <sup>-1</sup> )
EL/acetone 70:30	12.5	0.45	70.3	0.8	60	25–36	0.47	20	0.1–0.5
ML/acetone 70:30	12.5	0.43	96.4	0.8	60	34–35	0.37	20	0.1–0.5
CPO/EL/acetone 58:12:30	12.5	0.25	89.1	1.6	75	90–101	0.26	20	0.1–0.5
CPO/ML/acetone 58:12:30	12.5	0.25	102.9	1.6	75	65–71	0.27	20	0.1–0.5
DMF/acetone 80:20	16	0.40	139.6	0.2	75	95–101	0.15	20	0.1–0.5

<sup>a</sup> Polymer concentration in the solution

<sup>b</sup> Content of conductivity-enhancing additive BC per solution

Considering the different optimal process conditions (voltage and solution dosage) for each solvent system, the resulting nanofibre samples were compared on the basis of equal speed of

support textile movement. The basis weights and mean diameters of the nanofibres derived from each solution were determined for every speed at which the support was moved (Table 4 – selected speeds, Table S1 in Online Resource – all). The greatest basis weights for nanofibres were attained by the solvent systems based on either ethyl lactate or methyl lactate and acetone; they exceeded values observed for the DMF/acetone combination. However, the nanofibrous structures exhibiting the highest basis weights showed a tendency for layer cracking.

The DMF-based solvent system produced the thinnest fibres (116–150 nm). Among the nanostructures prepared from solutions with alternative solvents, those from cyclopentanone-based solutions were closest to these values. Fig. 3 presents SEM images of nanofibers prepared from the solutions in Table 3 with the distribution of fibre diameters of the layers electrospun at a support speed of 0.1 m min<sup>-1</sup> (the greatest basis weight).

Table 4 Structural properties of the nanofibrous layers

Ratio of solvents	Support fabric speed (m min <sup>-1</sup> )	Nanofibre properties	
		Basis weight (g m <sup>-2</sup> )	Mean fibre diameter (nm)
EL/acetone 70:30	0.1	2.16	268.54±113.15
	0.3	0.63	308.39±71.71
	0.5	0.38	351.01±108.82
ML/acetone 70:30	0.1	1.83	463.56±89.81
	0.3	0.55	488.80±105.70
	0.5	0.31	469.14±84.86
CPO/EL/acetone 58:12:30	0.1	1.47	156.89±41.63
	0.3	0.44	177.26±56.54
	0.5	0.24	188.43±65.17
CPO/ML/acetone 58:12:30	0.1	1.52	168.06±54.21
	0.3	0.47	168.06±43.19
	0.5	0.27	153.24±37.35
DMF/acetone 80:20	0.1	0.85	128.35±36.44
	0.3	0.26	117.31±30.82
	0.5	0.15	141.58±36.37

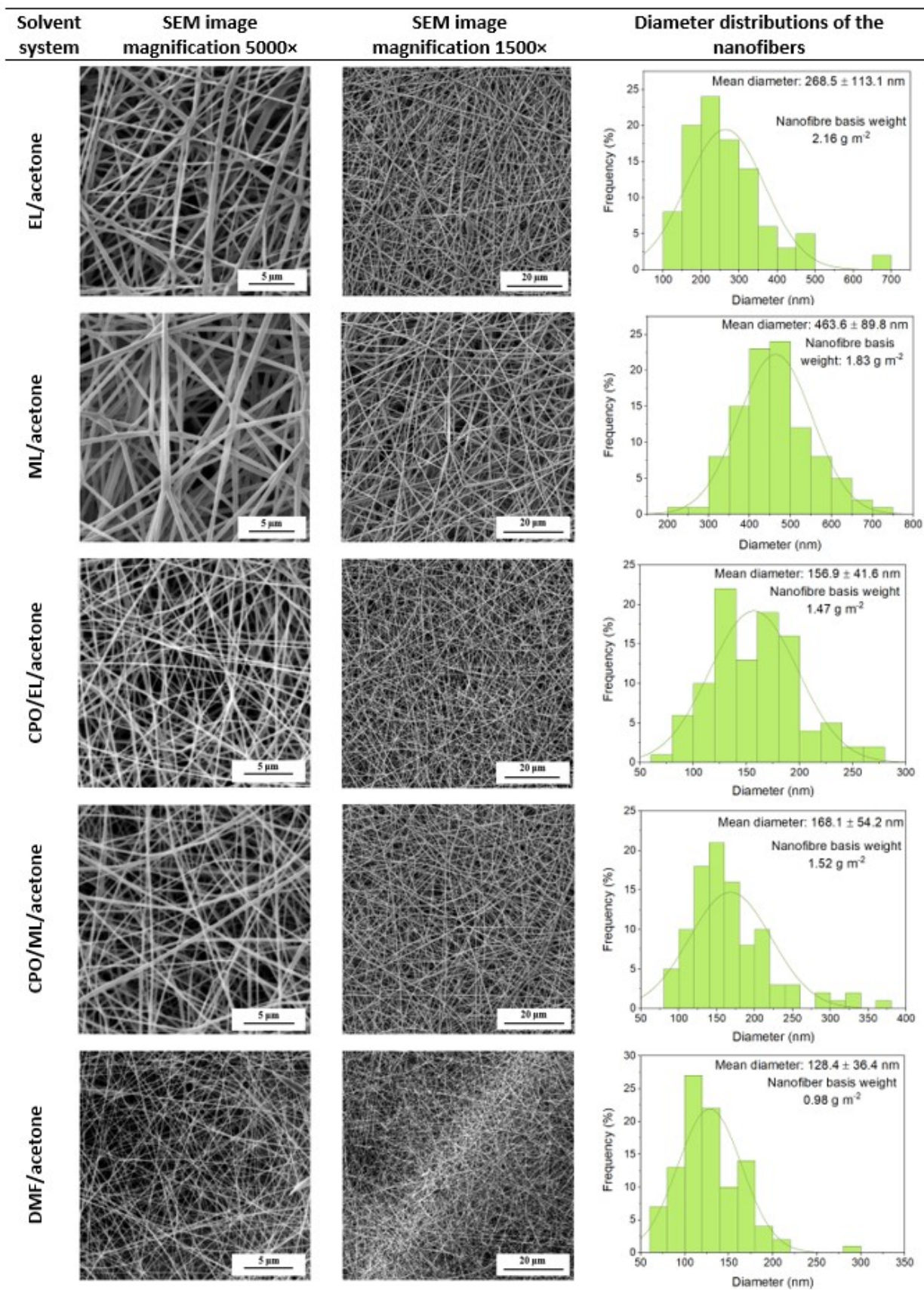


Fig. 3 SEM images and diameter distributions of nanofibers for PLA structures derived from different solvent systems and electrospun at the support speed of  $0.1 \text{ m min}^{-1}$

Fourier transform infrared spectroscopy was carried out to investigate possible changes in the material compositions of the nanofibre samples prepared from the various solutions (different solvent system) in addition to determining the presence of residual solvent in their structures. Comparison was made of the spectra of PLA virgin polymer (a pellet) and the PLA nanofibres (Fig. 4).

The spectrum plotted in red for the PLA pellet contains a band at  $1753\text{ cm}^{-1}$  attributed to the C=O stretching vibration of carboxyl groups. The peaks at  $1453$  and  $1381\text{ cm}^{-1}$  denote a vibration for CH bending deformation, whereas the two sharp peaks at  $1184$  and  $1087\text{ cm}^{-1}$  pertain to C-O stretching vibrations. The peak at  $2995\text{ cm}^{-1}$  relates to a CH stretching vibration [38–41].

Fig. 4 reveals that the spectra for the PLA pellet and nanofibres derived from the EL- or ML-based solutions are almost identical. However, those for samples prepared from the CPO/EL/acetone and CPO/ML/acetone solutions are broader in the region of  $1753\text{ cm}^{-1}$ , shifting the base of the peak to lower wavenumber, potentially because of the presence of solvents and their ester bands. This is confirming distinct shoulder visible in the region of  $1213\text{ cm}^{-1}$ , indicating the response to deformation of OH bands in the ML and EL. This could suggest presence of residual solvents.

As also evident from Fig. 4, the spectra of the PLA pellet and DMF/acetone-based PLA nanofibres differ notably. Since the given solvents exhibit very similar responses, it is not possible to distinguish them exactly. The differences in the spectra of the pellet and nanofibers are best visible in the CH vibration region at  $2927\text{ cm}^{-1}$ , the shoulder at  $1709\text{ cm}^{-1}$  and a new region at  $1258\text{ cm}^{-1}$ . These regions again confirm the possible presence of solvents in the nanofibrous material.

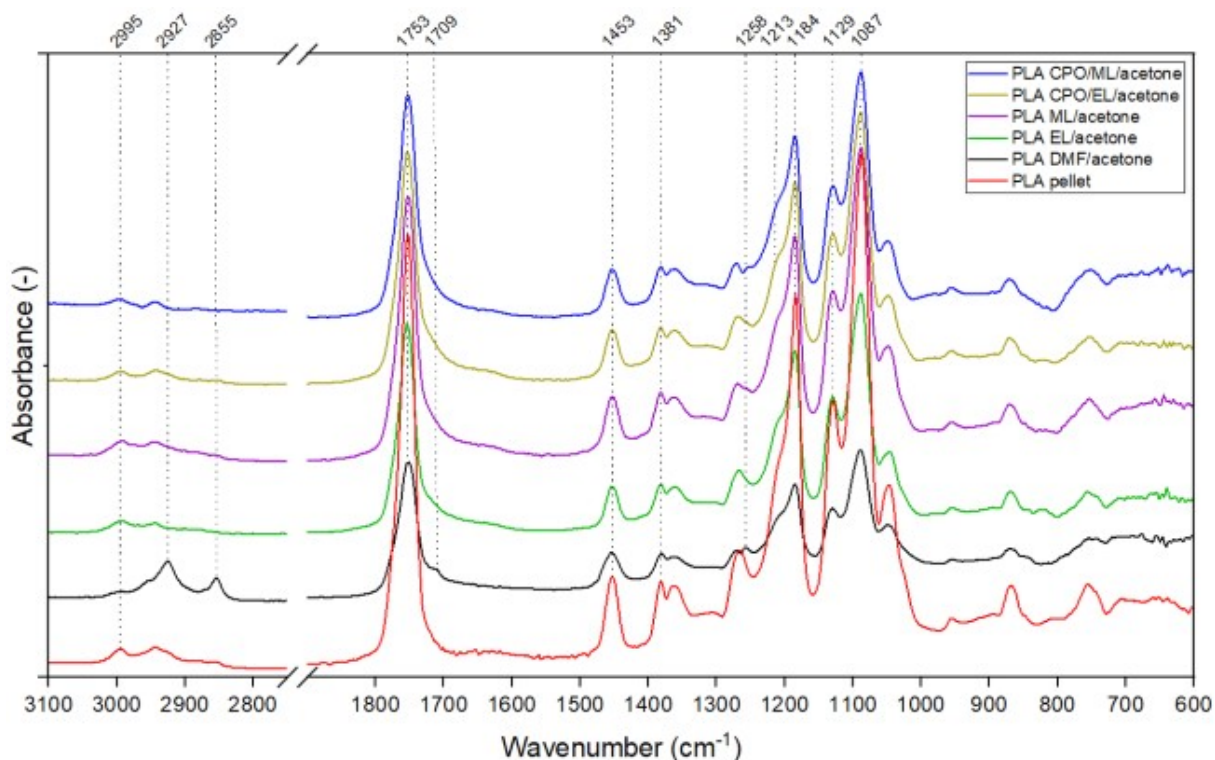


**Fig. 4** Fourier transform infrared (FTIR) spectra for a PLA pellet and the PLA nanofibres derived from each solvent system tested

Thermogravimetric analysis (TGA) was applied to determine the thermal stability and to confirm the possible presence of residual solvents of the various PLA nanofibres and reference pellet. As shown in Fig. 5, the PLA pellet exhibited a one-step loss in weight at an onset temperature of 290°C, with maximum decomposition occurring at 329°C. The residue remaining at the end of the heating cycle of the pellet amounted to less than 1%, indicating almost complete decomposition of the polymer. Unlike the virgin PLA, the nanofibres prepared from the EL, ML or CPO solvent systems demonstrated two stages of thermal loss in mass. As confirmed by FTIR, the first of these could be attributed to the evaporation and degradation of any residual green solvent present in the nanofibres, within the temperature range of 160-220°C. The most significant loss in mass occurred in the range of 30-200°C for the CPO/EL/acetone-based nanofibres. In the case of the DMF/acetone derived samples, no such initial loss was detected. The thermal degradation of PLA was observed at temperatures from 250°C to 330°C for all the nanofibrous materials.

The prepared nanofibre samples were subsequently conditioned to partially remove any residual solvent. This was carried out for 12 hours at 60°C in a vacuum oven to prevent destruction of the nanofibrous structures. The conditioning treatment had the effect of reducing loss in mass for every sample in the temperature range of 30-200°C (Fig. 5).

It is clear from the graphs in Fig. 5 (and Table S2 in Online Resource) that all the nanofibrous samples left a greater amount of final residue than the virgin PLA pellet (0.7% residue), even after conditioning. This was due to the presence of sodium tetraborate decahydrate in the nanofibres, which did not completely decompose during thermogravimetric analysis, accounting for more than 60% of the mass of the residue.

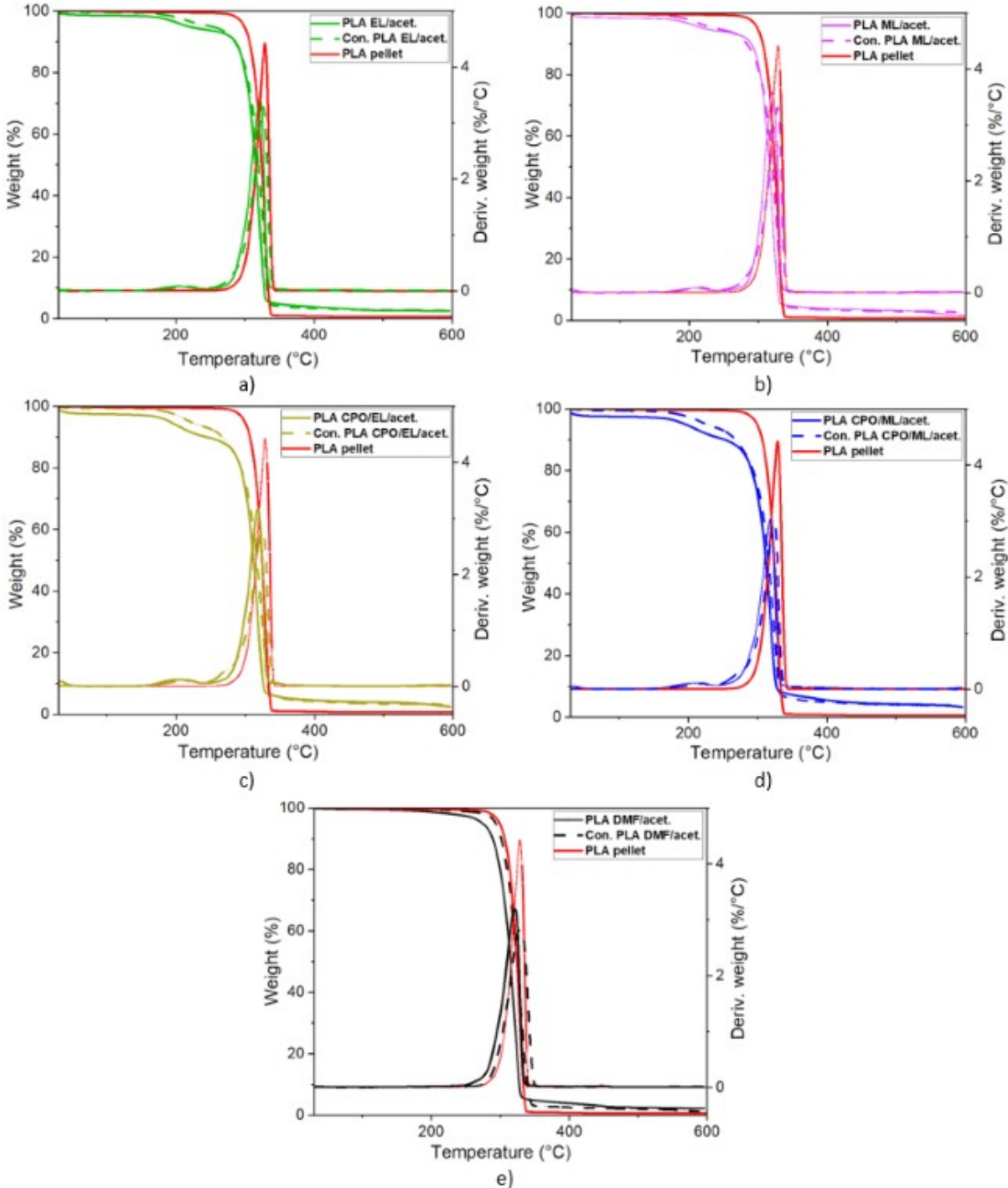


**Fig. 5** TGA plots for the various PLA nanofibres before and after conditioning, i.e., those based on the (a) EL/acetone, (b) ML/acetone, (c) CPO/EL/acetone, (d) CPO/ML/acetone and (e) DMF/acetone solvent systems; the plot in red is for the virgin PLA pellet

Both FTIR and thermogravimetric analyses indicated that an amount of residual solvent might be present in the nanofibrous materials prepared. Their presence in trace concentrations was confirmed by headspace solid-phase microextraction coupled with gas chromatography-mass spectrometry (HS-SPME-GC-MS), employing quadrupole time-of-flight mass spectrometry (Q-TOF). Despite the considerable sensitivity, it was necessary to use the deconvolution, when two substances with different spectra that are in coelution were distinguished. This made it possible to confirm the presence of trace amounts not only of the least evaporable solvent EL, but also of other solvents with relatively better evaporation (low relative evaporation rate ER - see Table 1), which are ML, CPO and even DMF. The only solvent that evaporated completely during the electrospinning process was acetone.

Surface wettability is an important property in some applications of membranes. Wettability is estimated by measuring the contact angle of a liquid, with distilled water being used as a test fluid to determine the hydrophilicity or hydrophobicity of the given material, i.e. its wettability to water.

Data on surface wettability of prepared nanofibre layers are expressed in terms of contact angle. Altering the solvent system brought about an insignificant reduction in contact angle values, from the maximum for PLA nanofibres prepared from the DMF/acetone solution ( $138.26 \pm 2.24^\circ$ ) to the minimum value of  $119.48 \pm 11.78^\circ$  for those resulting from the EL/acetone-based solution (for more details see table S3 in Online Resource). The conclusion was drawn that all the fabricated nanofibrous materials were hydrophobic in nature and changing the solvent did not markedly affect the wettability of the surface. Since no significant alteration in contact angle was witnessed, even when the basis weights of each set of nanofibrous materials was changed, it can be assumed that wettability was influenced rather by the nature of the polymer applied than the type of solvent.

In consideration of the prepared nanofibrous structures as an air filtration medium, a decisive factor for evaluation is their filtration efficiency. This is defined as the percentage of particles of a certain size that are stopped and retained by the filter medium, thereby determining the practical application of the membrane. Besides filtration efficiency, the pressure drop and particle size of the most penetrating particles (MPPS) are crucial aspects for a filtration material [42]. Capillary flow porometry was employed to determine the mean pore size (mean pore diameter) and pore size distribution for each nanofibrous material. The method is based on measurement of the pressure required to force air through a liquid-filled porous membrane [43]. The requirements for filter media are somewhat contradictory. The highest rated

materials are those that concurrently exhibit high filtration efficiency and low pressure drop. The filtration properties of nanofibrous media are influenced by several structural factors ranging from the thickness and arrangement of fibres in the nanofibrous layer to the basis weight of the material. It is logical that materials with a higher basis weight, prepared at lower speeds of the substrate movement, exhibit better filtration efficiency than materials with lower basis weights and larger pores between the nanofibres.

Table 5 lists the values gauged for the filtration properties and porosities of the nanofibrous materials prepared at different speeds of substrate movement (Table S1 in Online Resource contains data on all the speeds of substrate movement applied). The graphical comparison of the filtration properties and pore size distributions are shown in Fig. 6 and 7. The nanofibrous structure prepared from the DMF/acetone solution at the substrate speed of 0.1 m min<sup>-1</sup> possessed a filtration efficiency of 99.95%, whereas the material obtained from the CPO/EL/acetone-based solution at the same speed showed merely 0.3% less efficiency but with a lower pressure drop. The corresponding values of filtration efficiency for the CPO-based nanofibrous samples decreased quite sharply at higher speeds for substrate movement, in contrast to the DMF/acetone-based ones (Fig. 6).

Table 5 Filtration and porometry of the nanofibrous layers

Ratio of solvents	Support fabric speed (m min <sup>-1</sup> )	Filtration properties			Porometry
		Filtration efficiency (%)	Pressure drop (Pa)	MPPS (nm)	Mean pore size (µm)
EL/acetone 70:30	0.1	-	-	-	1.43±0.17
	0.3	79.9430	24.4	94.9	2.00±0.46
	0.5	73.5055	17.6	107.1	2.86±0.60
ML/acetone 70:30	0.1	92.4191	40.8	74.7	2.15±0.32
	0.3	70.6042	12.9	100.8	3.99±0.76
	0.5	66.7672	7.6	128.1	5.58±0.95
CPO/EL/acetone 58:12:30	0.1	99.6565	124.7	62.4	1.31±0.12
	0.3	78.9456	33.2	107.1	2.17±0.28
	0.5	66.9239	21.1	107.0	3.50±0.67
CPO/ML/acetone 58:12:30	0.1	99.5079	109.4	66.2	1.08±0.14
	0.3	93.0056	44.8	74.7	1.39±0.14
	0.5	71.9521	24.1	100.8	1.77±0.30
DMF/acetone 80:20	0.1	99.9512	153.4	46.3	0.79±0.08
	0.3	98.2053	48.6	46.3	0.91±0.06
	0.5	86.0228	2.4	74.7	1.45±0.15

The filtration properties of the prepared nanofibrous structures were determined in agreement with the EN 1822-1 standard for high efficiency air filters. This standard classifies filter materials under three groups according to filtration efficiency values: EPA filters – Efficiency Particulate Air filters (classes E10–12), HEPA filters – High Efficiency Particulate Air filters (classes H13–14) and ULPA filters – Ultra Low Particulate Air filters with very low penetration (classes U15–17).

The nanofibrous materials prepared from solutions in DMF/acetone and CPO/EL/acetone or CPO/ML/acetone at a substrate speed of  $0.1 \text{ m min}^{-1}$  can be rated as class H13, their filtration efficiency exceeding 99.95%. The DMF/acetone-based materials demonstrated a slight decrease in filtration efficiency with increasing substrate movement speed, meaning these materials prepared at such speeds were gradually classified as E11 and eventually E10. However, these materials could still be rated as high efficiency EPA filters.

In contrast, nanofibrous structures derived from the CPO/EL/acetone system exhibited a lesser filtration efficiency of 87.6%, corresponding to class E10, when the speed of substrate movement rose to  $0.2 \text{ m min}^{-1}$ . Increasing the velocity any further would render the resultant materials as unclassifiable as high efficiency filters.

The PLA nanofibrous materials prepared from the CPO/ML/acetone system showed (like the DMF/acetone ones) a gradual decrease in filtration efficiency in line with a rise in the speed of substrate movement (E11 at  $0.2 \text{ m min}^{-1}$  and E10 at  $0.3 \text{ m min}^{-1}$ ). Increasing it to  $0.4 \text{ m min}^{-1}$  brought about an almost 20% reduction in efficiency, hence materials fabricated under identical conditions or higher speed would no longer be classified as EPA filters. Although materials with low basis weights of nanofibres could not be classified as high efficiency filters, the gradual decrease in filtration efficiency observed for those with higher basis weights is a positive aspect and has the potential for practical application in manufacturing practice.

In connection with the measurement of the filtration properties, it should be further noted that the nanofibrous structure sample prepared from the PLA solution in the EL/acetone solvent system at the speed of textile substrate moving of  $0.1 \text{ m min}^{-1}$  could not be evaluated due to the insufficient mechanical properties of the sample. The prepared nanofibres were so fragile that the nanofibrous layer was always damaged – cracked during the measurements.

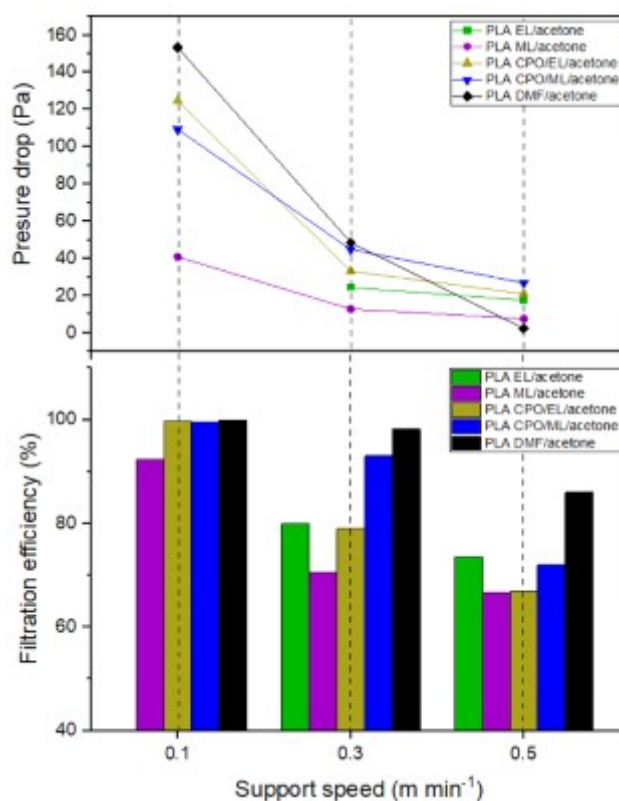


**Fig. 6** Comparison of filtration efficiency and pressure drop for nanofibrous membranes prepared from selected solvent systems, electrospun at different speeds of substrate movement

Of interest in this regard is comparison of the pore sizes and their distributions exhibited by three specific materials, namely nanostructures prepared from the solution with DMF/acetone and those where CPO was the primary solvent (CPO/EL/acetone and CPO/ML/acetone), as depicted in Fig. 7. The filtration efficiency for PLA nanofibres electrospun from solution with the DMF/acetone solvents demonstrated a very slow decrease. Raising the speed of substrate movement from  $0.1 \text{ m min}^{-1}$  to  $0.3 \text{ m min}^{-1}$  brought about a 2% drop in such efficiency; the mean pore size increased from  $0.79 \mu\text{m}$  to  $0.91 \mu\text{m}$ , while their distributions were very narrow and widths remained virtually unchanged (Fig. 7a). Samples derived from the CPO/acetone/EL system, in contrast, with identical increase in speed of substrate movement, showed significant widening in distribution of pore size. They also possessed a notable shift in mean pore size from  $1.31 \mu\text{m}$  for  $0.1 \text{ m min}^{-1}$  to  $2.17 \mu\text{m}$  at  $0.3 \text{ m min}^{-1}$ , which corresponded with a 20% decrease in filtration efficiency (Fig. 7c). The nanofibres prepared from the solution with the CPO/acetone/ML solvents, therefore, constitute a midway point between the two systems. The drop in filtration efficiency observed when heightening the speed from  $0.1$  to  $0.3 \text{ m min}^{-1}$  equalled approximately 6.5%, and the mean pore size shifted from  $1.08$  to  $1.39 \mu\text{m}$ ; the pore size distributions remained narrow (Fig. 7b).

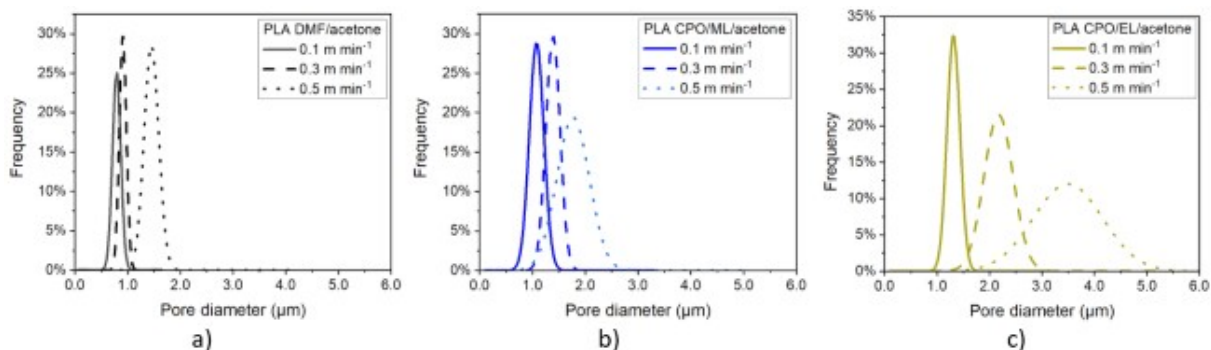


**Fig. 7** Comparison of pore size distributions of the PLA nanofibrous structures having the best filtration efficiencies based on the (a) DMF/acetone (b) CPO/ML/acetone and (c) CPO/EL/acetone solvent systems at different speeds of substrate movement

The presented results show that nanofibrous materials can be prepared from green solvent-based solutions of CPO/EL/acetone or CPO/ML/acetone, which exhibit good filtration properties comparable to those prepared from DMF/acetone-based solutions. This is especially relevant for nanofibrous layers prepared at a minimum collection substrate speed of  $0.1 \text{ m min}^{-1}$  (class H13 according to EN1822-1). The electrospinning process of PLA from CPO/EL/acetone and CPO/ML/acetone produces non-defective fibres with a slightly greater thickness of fibres than that from DMF/acetone. The process is also somewhat more efficient, and therefore the basis weight of the materials prepared from ternary solvents is 42% (CPO/EL/acetone) and 44% (CPO/ML/acetone) higher than that of the PLA nanofibers from DMF/acetone, which contributes to the high filtration efficiency. Although the larger fibre thickness generates larger pore sizes for materials with CPO as the main solvent ( $1.31 \mu\text{m}$  for CPO/EL/acetone,  $1.08 \mu\text{m}$  for CPO/ML/acetone and  $0.79 \mu\text{m}$  for DMF/acetone), the good homogeneity of the nanofibrous layers ensures a narrow pore size distribution. As a result, the pressure drop of CPO/EL/acetone and CPO/ML/acetone based nanofibrous membranes is lower than that of DMF/acetone based PLA membrane.

#### 4. Conclusion

This research focused on the identification of suitable alternative solvents for the preparation of polymer solutions for the fabrication of PLA nanofibres by electrospinning. The main objective was to replace DMF, a toxic organic solvent that has an impact on human health and the environment, with more acceptable types of so-called green solvents. The need to find

alternatives to highly toxic solvents is also amplified and accelerated by the concerns about REACH legislation and associated restrictions.

In the study, the selection of suitable solvent alternatives for the preparation of PLA polymer solutions and the optimization of nanofibre preparation by electrospinning were carried out. The choice of green solvents was primarily limited by a crucial parameter, namely the evaporation rate. Another issue concerned the solubility of a conductivity-enhancing agent that was added into the polymer solution. In this context, it has been proved that a single solvent is not sufficient and a combination of solvents is required. The PLA nanofibers electrospun mainly from ternary solvents CPO/EL/acetone and CPO/ML/acetone exhibited properties similar to those prepared from DMF/acetone-based solution. Non-defective nanofibers with comparable morphology of the nanofibrous layer, but mainly with comparable filtration efficiency and even slightly lower pressure drop were prepared, which is especially pronounced for materials with higher basis weight.

In conclusion, there is a real possibility of upscaling the electrospinning of PLA nanofibers from a green ternary solvent system to industrial production of nanofibrous air filtration membranes. The added value to the good electrospinnability of these solutions is the reduced health and environmental risk, which will help to meet legislative conditions, but also economic feasibility and recyclability. These are significant advantages for both production and companies' waste management processes.

### **Acknowledgements**

This research was supported by the Ministry of Education Youth and Sports of the Czech Republic – programme DKRVO RP/CPS/2024–28/002.

### **Author contributions**

L.L. contributed to conception and planning of the work, L.L. and M.K. contributed by drafting and critical revision of the manuscript and they provided analysis and interpretation of the data, D.H., A.P. and D.K. provided analysis, V.S. approved the final submitted version of the manuscript.

### **Declaration of competing interest**

The authors declare no conflict of interest.

### **Data and code availability**

Not Applicable.

## Supplementary information

This manuscript is supplemented by a document containing data on the full range of samples tested (ESR\_1).

## Ethical approval

Not Applicable.

## References

1. Xue J, Wu T, Dai Y, Xia Y (2019) Electrospinning and Electrospun Nanofibers: Methods, Materials, and Applications. *Chem Rev* 119:5298–5415. <https://doi.org/10.1021/acs.chemrev.8b00593>
2. Wu J-H, Hu T-G, Wang H, et al (2022) Electrospinning of PLA Nanofibers: Recent Advances and Its Potential Application for Food Packaging. *J Agric Food Chem* 70:8207–8221. <https://doi.org/10.1021/acs.jafc.2c02611>
3. El-Aassar MR, Ibrahim OM, Al-Oanzi ZH (2021) Biotechnological Applications of Polymeric Nanofiber Platforms Loaded with Diverse Bioactive Materials. *Polymers* 13:3734. <https://doi.org/10.3390/polym13213734>
4. Imani F, Karimi-Soflou R, Shabani I, Karkhaneh A (2021) PLA electrospun nanofibers modified with polypyrrole-grafted gelatin as bioactive electroconductive scaffold. *Polymer* 218:123487. <https://doi.org/10.1016/j.polymer.2021.123487>
5. Gao H, Liu G, Guan J, et al (2023) Biodegradable hydro-charging polylactic acid melt-blown nonwovens with efficient PM0.3 removal. *Chem Eng J* 458:141412. <https://doi.org/10.1016/j.cej.2023.141412>
6. Zhou Y, Liu Y, Zhang M, et al (2022) Electrospun Nanofiber Membranes for Air Filtration: A Review. *Nanomaterials* 12:1077. <https://doi.org/10.3390/nano12071077>
7. Fan T, Daniels R (2021) Preparation and Characterization of Electrospun Polylactic Acid (PLA) Fiber Loaded with Birch Bark Triterpene Extract for Wound Dressing. *AAPS PharmSciTech* 22:205. <https://doi.org/10.1208/s12249-021-02081-z>
8. Biswas MC, Jony B, Nandy PK, et al (2022) Recent Advancement of Biopolymers and Their Potential Biomedical Applications. *J Polym Environ* 30:51–74. <https://doi.org/10.1007/s10924-021-02199-y>
9. Wu Y, Wang Y, Wang F, et al (2022) Preparation and properties study of polylactic acid/bacterial cellulose composite scaffolds by solvent removal. *Journal of Materials Research* 37:1602–1611. <https://doi.org/10.1557/s43578-022-00560-y>
10. He X-X, Zeng J, Yu G-F, et al (2017) Near-Field Electrospinning: Progress and Applications. *J Phys Chem C* 121:.. <https://doi.org/10.1021/acs.jpcc.6b12783>
11. Zubir AAM, Khairunnisa MP, Surib NA, et al (2020) Electrospinning of PLA with DMF: Effect of polymer concentration on the bead diameter of the electrospun fibre.

IOP Conf Ser: Mater Sci Eng 778:012087.  
<https://doi.org/10.1088/1757-899X/778/1/012087>

12. Ji K, Liu C, He H, et al (2023) Green-Solvent-Processable Composite Micro/Nanofiber Membrane with Gradient Asymmetric Structure for Efficient Microfiltration. *Small* 19:2207330. <https://doi.org/10.1002/sml.202207330>
13. Mu J, Pei X, Dai W, et al (2021) A Novel Biodegradable Fibrous Membrane with Remarkable Filtration and Antibacterial Properties. *J Polym Environ* 29:4040–4047. <https://doi.org/10.1007/s10924-021-02163-w>
14. Casasola R, Thomas NL, Trybala A, Georgiadou S (2014) Electrospun poly lactic acid (PLA) fibres: Effect of different solvent systems on fibre morphology and diameter. *Polymer* 55:4728–4737. <https://doi.org/10.1016/j.polymer.2014.06.032>
15. Casalini T, Rossi F, Castrovinci A, Perale G (2019) A Perspective on Polylactic Acid-Based Polymers Use for Nanoparticles Synthesis and Applications. *Front Bioeng Biotechnol* 7:259. <https://doi.org/10.3389/fbioe.2019.00259>
16. Jash A, Paliyath G, Lim L-T (2018) Activated release of bioactive aldehydes from their precursors embedded in electrospun poly(lactic acid) nonwovens. *RSC Adv* 8:19930–19938. <https://doi.org/10.1039/C8RA03137A>
17. Jordan A, Hall CGJ, Thorp LR, Sneddon HF (2022) Replacement of Less-Preferred Dipolar Aprotic and Ethereal Solvents in Synthetic Organic Chemistry with More Sustainable Alternatives. *Chem Rev* 122:6749–6794. <https://doi.org/10.1021/acs.chemrev.1c00672>
18. Xie W, Li T, Tiraferri A, et al (2021) Toward the Next Generation of Sustainable Membranes from Green Chemistry Principles. *ACS Sustainable Chem Eng* 9:50–75. <https://doi.org/10.1021/acssuschemeng.0c07119>
19. Avossa J, Herwig G, Toncelli C, et al (2022) Electrospinning based on benign solvents: current definitions, implications and strategies. *Green Chem* 24:2347–2375. <https://doi.org/10.1039/D1GC04252A>
20. Byrne FP, Jin S, Paggiola G, et al (2016) Tools and techniques for solvent selection: green solvent selection guides. *Sustain Chem Process* 4:7. <https://doi.org/10.1186/s40508-016-0051-z>
21. Amelio A, Genduso G, Vreysen S, et al (2014) Guidelines based on life cycle assessment for solvent selection during the process design and evaluation of treatment alternatives. *Green Chem* 16:3045–3063. <https://doi.org/10.1039/C3GC42513D>
22. Prat D, Wells A, Hayler J, et al (2015) CHEM21 selection guide of classical- and less classical-solvents. *Green Chem* 18:288–296. <https://doi.org/10.1039/C5GC01008J>
23. Henderson RK, Jiménez-González C, Constable DJC, et al (2011) Expanding GSK's solvent selection guide – embedding sustainability into solvent selection starting at medicinal chemistry. *Green Chem* 13:854–862. <https://doi.org/10.1039/C0GC00918K>

24. Kim H-B, Yoo J-I, Kang S-C, Song J-K (2024) Green Solvent Selection for All Solution-Processed Inverted Quantum Dot Light Emitting Diode. *Small* 20:2304051. <https://doi.org/10.1002/sml.202304051>
25. Kahrs C, Schwellenbach J (2020) Membrane formation via non-solvent induced phase separation using sustainable solvents: A comparative study. *Polymer* 186:122071. <https://doi.org/10.1016/j.polymer.2019.122071>
26. Naziri Mehrabani SA, Vatanpour V, Koyuncu I (2022) Green solvents in polymeric membrane fabrication: A review. *Sep Purif Technol* 298:121691. <https://doi.org/10.1016/j.seppur.2022.121691>
27. Cardoso AP, Giacobbo A, Bernardes AM, Ferreira CA (2024) Performance evaluation of polysulfone-based membranes produced with a green solvent. *Journal of Materials Research* 39:1525–1536. <https://doi.org/10.1557/s43578-024-01327-3>
28. Clarke CJ, Tu W-C, Levers O, et al (2018) Green and Sustainable Solvents in Chemical Processes. *Chem Rev* 118:747–800. <https://doi.org/10.1021/acs.chemrev.7b00571>
29. Mosher CZ, Brudnicki PAP, Gong Z, et al (2021) Green electrospinning for biomaterials and biofabrication. *Biofabrication* 13:. <https://doi.org/10.1088/1758-5090/ac0964>
30. Kim D, Nunes SP (2021) Green solvents for membrane manufacture: Recent trends and perspectives. *Curr Opin Green Sustain Chem* 28:100427. <https://doi.org/10.1016/j.cogsc.2020.100427>
31. Lopez J, Pletscher S, Aemissegger A, et al (2018) N-Butylpyrrolidinone as Alternative Solvent for Solid-Phase Peptide Synthesis. *Org Process Res Dev* 22:494–503. <https://doi.org/10.1021/acs.oprd.7b00389>
32. Duereh A, Sato Y, Smith RL Jr, Inomata H (2017) Methodology for Replacing Dipolar Aprotic Solvents Used in API Processing with Safe Hydrogen-Bond Donor and Acceptor Solvent-Pair Mixtures. *Org Process Res Dev* 21:114–124. <https://doi.org/10.1021/acs.oprd.6b00401>
33. Inamuddin, Boddula R, Ahamed MI, Asiri AM (2020) Green sustainable process for chemical and environmental engineering and science: solvents for the pharmaceutical industry, 1st ed. Elsevier Publications, Cambridge
34. Alder CM, Hayler JD, Henderson RK, et al (2016) Updating and further expanding GSK's solvent sustainability guide. *Green Chem* 18:3879–3890. <https://doi.org/10.1039/C6GC00611F>
35. Casasola R, Thomas NL, Georgiadou S (2016) Electrospinning of poly(lactic acid): Theoretical approach for the solvent selection to produce defect-free nanofibers. *J Polym Sci, Part B: Polym Phys* 54:1483–1498. <https://doi.org/10.1002/polb.24042>
36. Song J, Zhang B, Lu Z, et al (2019) Hierarchical Porous Poly(l-lactic acid) Nanofibrous Membrane for Ultrafine Particulate Aerosol Filtration. *ACS Appl Mater Interfaces* 11:46261–46268. <https://doi.org/10.1021/acsami.9b18083>

37. Maleki H, Azimi B, Ismaeilimoghadam S, Danti S (2022) Poly(lactic acid)-Based Electrospun Fibrous Structures for Biomedical Applications. *Appl Sci* 12:3192. <https://doi.org/10.3390/app12063192>
38. Auras R, Harte B, Selke S (2004) An Overview of Polylactides as Packaging Materials. *Macromolecular Bioscience* 4:835–864. <https://doi.org/10.1002/mabi.200400043>
39. George Socrates (2004) *Infrared and Raman Characteristic Group Frequencies: Tables and Charts*, 3rd Edition, 3rd ed. John Wiley & Sons
40. Liu H, Zhao R, Song X, et al (2017) Lewis Acidic Ionic Liquid [Bmim]FeCl<sub>4</sub> as a High Efficient Catalyst for Methanolysis of Poly (lactic acid). *Catal Lett* 147:2298–2305. <https://doi.org/10.1007/s10562-017-2138-x>
41. Milaniak N, Laroche G, Massines F (2021) Fourier-transform infrared spectroscopy of ethyl lactate decomposition and thin-film coating in a filamentary and a glow dielectric barrier discharge. *Plasma Process Polym* 18:2000248. <https://doi.org/10.1002/ppap.202000248>
42. Riccardis D, Federica M (2023) Electrospun Nanofibrous Membranes for Air Filtration: A Critical Review. *Compouds* 3:390–410. <https://doi.org/10.3390/compounds3030030>
43. Agarwal C, Pandey AK, Das S, et al (2012) Neck-size distributions of through-pores in polymer membranes. *J Membr Sci* 415–416:608–615. <https://doi.org/10.1016/j.memsci.2012.05.055>